

# One- and Two-Dimensional MAS $^{13}\text{C}$ NMR Analyses of Molecular Motions in Poly(2-hydroxypropyl Ether of Bisphenol-A)

Hironori Kaji,\* Toshihiro Tai,<sup>†</sup> and Fumitaka Horii\*

Institute for Chemical Research, Kyoto University, Uji, Kyoto 611-0011, Japan

Received March 13, 2001

**ABSTRACT:** The dynamics of amorphous poly(2-hydroxypropyl ether of bisphenol-A) (PHR), quenched from the melt, has been investigated by one- and two-dimensional solid-state  $^{13}\text{C}$  NMR spectroscopy. CP/MAS and dipolar decoupled/MAS  $^{13}\text{C}$  NMR spectra from  $-150$  to  $180$  °C give two specific features: (1) below  $23$  °C, resonance lines for C–H carbons of phenylene rings split into two lines; (2) line widths of resonance lines become broad at  $110$ – $140$  °C ( $30$ – $60$  °C above the glass transition temperature). Feature 1 indicates that phenylene C–H carbons exist in two magnetically different sites at low temperatures. These two sites are associated with asymmetric conformational states, which may be produced by  $\text{OH}\cdots\pi$  hydrogen bond formation. The coalescence of the resonance lines at elevated temperatures is caused by the  $\pi$  flip motion of phenylene rings, which corresponds to the  $\gamma$  relaxation for PHR. The correlation time of the  $\pi$  flip motion is analyzed by the two-site exchange model and is found to follow the Arrhenius equation. The apparent activation energy is  $51\text{ kJ mol}^{-1}$  by assuming an inhomogeneous correlation time distribution described by a Kohlrausch–Williams–Watts (KWW) function with an exponent of  $0.2$ . Feature 2 is caused by the so-called motional broadening, which is originated by enhanced segmental motions. This dynamics corresponds to the  $\alpha$  relaxation for PHR and can be described by the William–Landel–Ferry (WLF) equation. Two-dimensional (2D) CP/MAS  $^{13}\text{C}$  exchange NMR experiments confirm the existence of flip angle distribution as well as the distribution of correlation times of the phenylene ring  $\pi$  flip motion. The 2D experiments at  $-120$  °C confirm the KWW exponent of  $0.2$ .

## Introduction

Poly(2-hydroxypropyl ether of bisphenol-A), known as phenoxy resin (PHR), is an amorphous linear polymer, and the structure and dynamics have been studied by X-ray diffraction,<sup>1</sup> mechanical relaxation,<sup>2,3</sup> and solid-state NMR methods.<sup>4,5</sup> On mechanical relaxation experiments, Takahama et al.<sup>2</sup> observed a relaxation between  $-100$  and  $-40$  °C. Erro et al.<sup>3</sup> carried out mechanical relaxation experiments with a wider temperature range and found three relaxations at  $-100$  to  $-40$ ,  $20$ – $40$ , and  $70$ – $100$  °C. For the lowest relaxation, there is no common notation: Takahama et al.<sup>2</sup> and Shi et al.<sup>5</sup> called it  $\beta$  relaxation, while Erro et al.<sup>3</sup> called it  $\gamma$  relaxation because they found other two relaxations at higher temperatures. In this article, we call the lowest relaxation the  $\gamma$  relaxation for PHR.

Up to now, many researches have been carried out to elucidate the molecular origin of the  $\gamma$  relaxation. Recently, Shi et al.<sup>5</sup> carried out solid-state  $^2\text{H}$  NMR experiments both for phenylene ring deuterated PHR samples and methylene unit deuterated PHR samples to clarify the molecular-level origin of the  $\gamma$  relaxation. From these  $^2\text{H}$  NMR experiments, it was found that the lower and higher temperature parts of the  $\gamma$  relaxation were attributed to  $\pi$  flip motion of phenylene rings and motion of hydroxy ether groups, respectively, although all the relaxation envelopes could not be explained only by these two mechanisms. The temperature range, where  $^2\text{H}$  NMR spectra were analyzed, was from  $+70$  to  $-20$  °C, and the analyzed correlation times were  $10^{-7}$ – $10^{-4}$  s. They extrapolated these data to a much longer correlation time,  $1$  s, to compare with mechanical

relaxation data. Furthermore, the temperature range of the  $^2\text{H}$  NMR analysis overlapped with that of the  $\beta$  relaxation at  $20$ – $40$  °C, as described above. To confirm the structural source of the  $\gamma$  relaxation, site-selective experiments are required on time scales of about  $1$  s or at the temperature range around  $-100$  to  $-40$  °C.

In this paper, we measure CP/MAS  $^{13}\text{C}$  NMR spectra and analyze them by the two-site exchange model. Fortunately, drastic changes of line shapes are observed at the temperature range from  $-150$  to  $23$  °C, which covers that of the mechanical  $\gamma$  relaxation. Thus, the analyzed data can be compared with mechanical relaxation data without extrapolation. It is also favorable that we do not need to think of the overlap with the  $\beta$  relaxation. We also carry out two-dimensional (2D) CP/MAS  $^{13}\text{C}$  exchange NMR experiments, which provide information on dynamics on the time scale comparable to the mechanical relaxation experiments. In the analyses of one-dimensional (1D) CP/MAS  $^{13}\text{C}$  NMR spectra or  $^2\text{H}$  NMR spectra, the breadth of the correlation time distribution is a crucial factor because it greatly affects the apparent activation energy of the relevant motion. The 2D experiments can reveal the breadth of the correlation time distribution, which cannot be analyzed uniquely, not only from 1D CP/MAS  $^{13}\text{C}$  NMR spectra but also from  $^2\text{H}$  NMR spectra. The dynamics of the  $\alpha$  relaxation is also characterized by the analysis of motional broadening in CP/MAS and dipolar decoupled (DD)/MAS  $^{13}\text{C}$  NMR experiments at  $80$ – $180$  °C.

## Experimental Section

**Sample.** Phenoxy resin (PHR) films, (Union Carbide, grade PKHJ), used in this work, were prepared by being hot-pressed at  $160$  °C under  $100\text{ kg cm}^{-2}$ , quenched in ice–water, and dried at room temperature under vacuum for  $3$  days.

**NMR Measurements.** Solid-state  $^{13}\text{C}$  NMR measurements were conducted on a Chemagnetics CMX-400 spectrometer

\* Corresponding authors.

<sup>†</sup> Current address: Daicel Chemical Industries, Ltd., 1, Teppo Cho, Sakai, Osaka 590-0905, Japan.

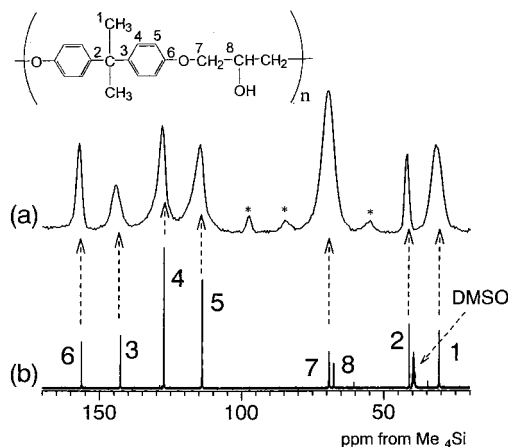


**Figure 1.** 100 MHz  $^{13}\text{C}$  NMR spectra of phenoxy resin (PHR): (a) CP/MAS spectrum at 23 °C; (b) solution-state spectrum at 100 °C. The sign \* indicates spinning sidebands.

operating under a static magnetic field of 9.4 T. The  $^1\text{H}$  and  $^{13}\text{C}$  field strengths  $\gamma B_1/2\pi$  of 62.5 kHz were used for 90° pulses and the cross polarization (CP). The contact time for the CP process was 2.0 ms. The dwell time and the acquisition time were 16.67  $\mu\text{s}$  and 17.07 ms, respectively. CP/MAS spectra were measured at  $-150$  to  $+150$  °C. At 180 °C, the DD/MAS spectrum was measured, which gives better signal/noise ratio. To avoid the arcing problem at this wide temperature range, the  $^1\text{H}$  field strength during the dipolar decoupling was reduced to 50.0 kHz for all the experiments. The temperatures appeared in this paper were the calibrated temperatures by the ethylene glycol method.<sup>6,7</sup>  $^{13}\text{C}$  chemical shifts were expressed as values relative to tetramethylsilane ( $\text{Me}_4\text{Si}$ ) by using the  $\text{CH}_3$  resonance line at 17.36 ppm for hexamethyl benzene crystals as an external reference. The rate of sample spinning was set to 6 kHz throughout this work.

Solution-state  $^{13}\text{C}$  NMR measurements were conducted on a JEOL JNM-GX 400 spectrometer operating under a static magnetic field of 9.4 T.  $\text{DMSO}-d_6$  was used as a solvent, and measurements were carried out at 100 °C. The assignment of the solution spectrum is confirmed by the incredible natural abundance double quantum transfer experiment (INADEQUATE). The pulse sequence is  $90^\circ - \tau_{\text{DQ}} - 180^\circ - \tau_{\text{DQ}} - 90^\circ - t_1 - 135^\circ$ . The  $^{13}\text{C}$  field strengths  $\gamma B_1/2\pi$  of 10.4 kHz were used for 90°, 180°, and 135° pulses. The acquisition time and  $\tau_{\text{DQ}}$  were 68 and 5 ms, respectively. In the  $t_1$  dimension, 64 slices with increments of 33  $\mu\text{s}$  were acquired.

**Differential Scanning Calorimetry (DSC).** DSC measurements were performed on a TA Instruments DSC 2910 differential scanning calorimeter. Indium was used as a standard for temperature calibration. The glass transition temperature ( $T_g$ ) determined from an onset temperature of a DSC curve at a heating rate of 10 °C/min was 80 °C for PHR. No other obvious exothermic and endothermic peaks were observed between  $-100$  and 200 °C.

## Results and Discussion

**CP/MAS  $^{13}\text{C}$  NMR Spectra.** Figure 1a shows a CP/MAS  $^{13}\text{C}$  NMR spectrum of PHR at 23 °C. The assignment of each resonance line has been made on the basis of a result of a solution-state  $^{13}\text{C}$  NMR spectrum shown in Figure 1b. Figure 2 shows CP/MAS and DD/MAS  $^{13}\text{C}$  NMR spectra of PHR at different temperatures ranging from  $-150$  to 180 °C. We can find two interesting features: One feature is that the resonance lines for C-H carbons of phenylene rings split into two resonance lines below 23 °C. This indicates that the phenylene C-H carbons exist in magnetically different two sites at lower temperatures and the coalescence of the resonance lines is caused by some phenylene ring motion, as characterized in detail below. The temper-

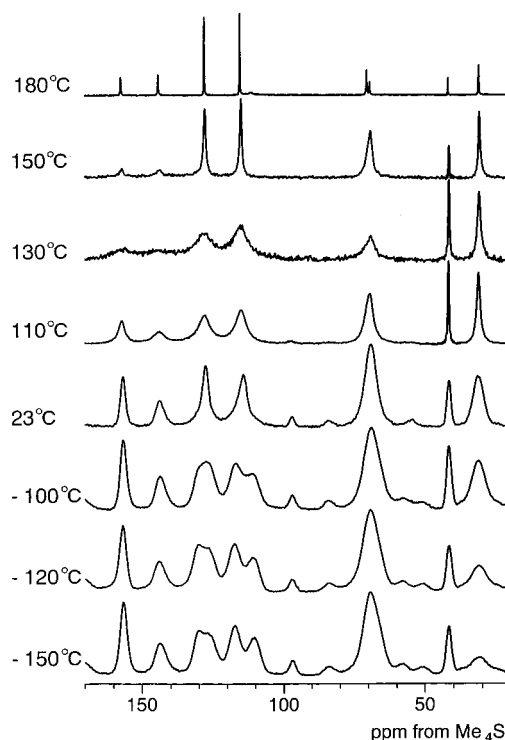


**Figure 2.** CP/MAS  $^{13}\text{C}$  NMR spectra of PHR from  $-150$  to 150 °C and DD/MAS  $^{13}\text{C}$  NMR spectrum of PHR at 180 °C.

ature range of this relaxation appearing from  $-120$  to  $-20$  °C corresponds to the  $\gamma$  relaxation observed by mechanical relaxation measurements.<sup>2,3</sup> The other feature in Figure 2 is that the line widths become broad at 110–140 °C ( $T_g + 30 - T_g + 60$  °C), which is caused by enhanced molecular motion.<sup>8–11</sup> This process corresponds to the  $\alpha$  relaxation.

**Two-Site Exchange Analysis.** At temperatures below 23 °C, the resonance lines for C5 carbons split into two peaks, as described above. This type of splitting of resonance lines is already observed for cured epoxy resins.<sup>12</sup> The chemically different two sites in C5 carbons are produced by asymmetric conformational states, which may be caused by an  $\text{OH} \cdots \pi$  hydrogen bond<sup>13–15</sup> between the hydroxyl group and the phenylene ring. This effect becomes clear when we compare the CP/MAS  $^{13}\text{C}$  NMR spectra of PHR with those for polycarbonate of bisphenol-A (PC), which has no hydroxyl group. Figure 3 shows CP/MAS  $^{13}\text{C}$  NMR spectra of PC at  $-150$  to 25 °C. This figure and the figure in ref. 16 show that no obvious line splitting is observed for C-H phenylene ring carbons of PC. It is therefore found that there exists some stronger interaction between phenylene rings and hydroxyl groups in PHR.

With increasing temperature, these resonance lines in PHR begin to coalesce around  $-100$  °C and finally become a single peak at 23 °C. As is shown below, the coalescence of resonance lines arises from  $\pi$  flip motion of phenylene rings. The correlation time of the  $\pi$  flip motion is analyzed by using the two-site exchange model<sup>17,18</sup> under an assumption that the phenylene ring motion is frozen at  $-150$  °C.

According to the two-site exchange theory,<sup>17,18</sup> the resonance line  $I(\omega)$  can be described as

$$I(\omega) = \frac{1}{2} \frac{\kappa(\omega_1 - \omega_2)^2}{(\omega - \omega_1)^2(\omega - \omega_2)^2 + \kappa^2[2\omega - (\omega_1 + \omega_2)]^2} \quad (1)$$

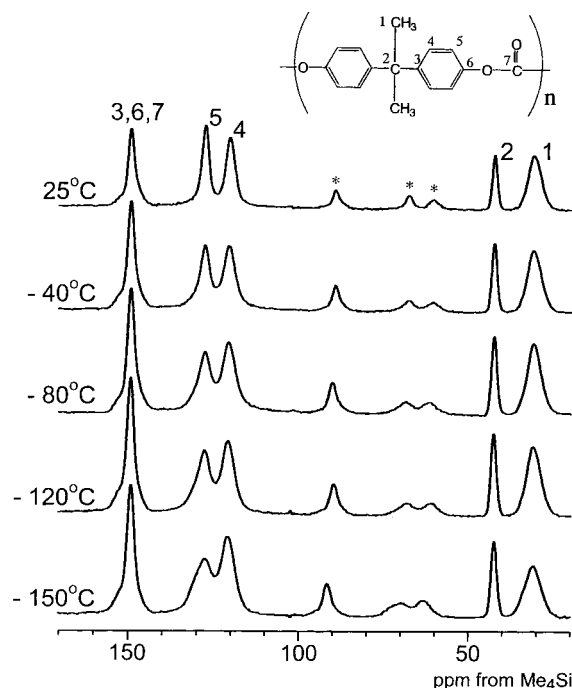


**Figure 3.** CP/MAS  $^{13}\text{C}$  NMR spectra of polycarbonate of bisphenol-A (PC) at different temperatures.

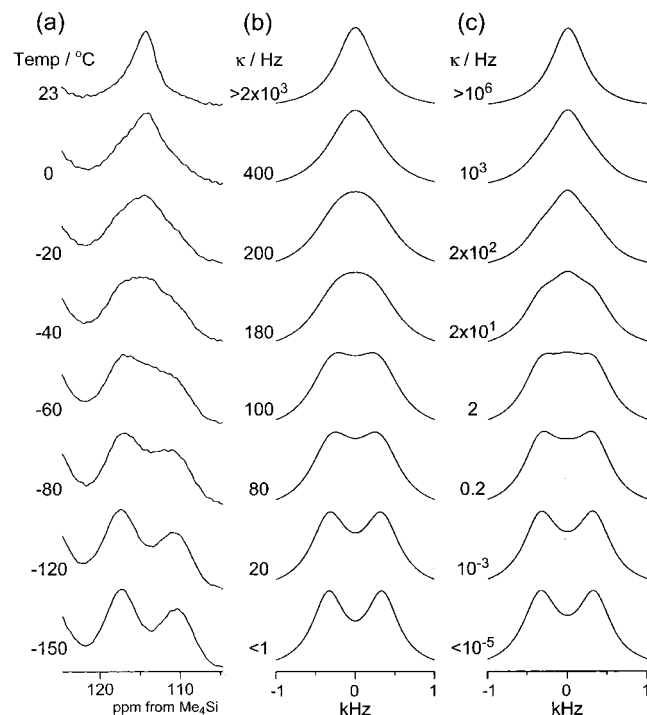


**Figure 4.** Motional exchange line shapes for CP/MAS  $^{13}\text{C}$  NMR spectra of the C5 carbon at different temperatures: experimental (a) and simulated in terms of the two-site exchange model, where KWW distributions of correlation times are assumed to be  $\beta = 1.0$  (single correlation time) (b) and 0.2 (c).

where  $\omega_1$  and  $\omega_2$  are resonance frequencies in the respective sites and  $\kappa$  is the rate of the exchange motion. In the actual calculation,  $(\omega_1 - \omega_2)/2\pi$  is set to be 680 Hz, and Lorentzian broadening of 180 Hz is applied.

Figure 4b shows the simulated resonance line shapes for C5 carbons and the corresponding rates of the exchange motion. A single rate of the motion is assumed for the analyses. The experimental line shapes in Figure 4a are well reproduced by the simulation as shown in

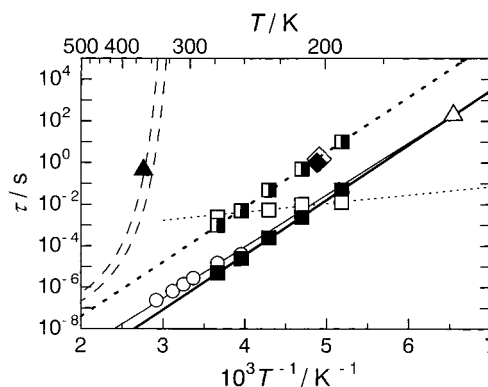


**Figure 5.** Arrhenius plot for the correlation time of motion associated with the  $\alpha$  and  $\gamma$  relaxations of PHR. Broken lines, motional broadening;  $\blacktriangle$ , 2D exchange at 90 °C;  $\triangle$ , 2D exchange at -120 °C;  $\square$  and thin dotted line, two-site exchange with KWW  $\beta = 1.0$  (single correlation time);  $\blacksquare$  and thick dotted line, two-site exchange with KWW  $\beta = 0.2$ ;  $\blacksquare$  and thick solid line, two-site exchange with KWW  $\beta = 0.2$  in which flip angle distributions are considered according to the result of 2D exchange;  $\circ$  and thin solid line,  $^2\text{H}$  NMR; $^5$   $\blacklozenge$ , dynamic mechanical analysis; $^3$   $\diamond$ , torsion pendulum. $^2$

Figure 4b. The correlation times, which are defined as  $\tau = \kappa^{-1}$ , obtained by this analysis, are plotted against inverse absolute temperatures as open squares in Figure 5. The temperature dependence of the correlation times is found to follow the Arrhenius equation, the apparent activation energy being 7.8 kJ mol $^{-1}$ . This value is quite lower than the apparent activation energy previously reported for the  $\pi$  flip motion of phenylene groups for several polymers containing bisphenol-A residues; for example, 48 kJ mol $^{-1}$  was obtained by the  $^2\text{H}$  NMR analysis of PHR, $^5$  50 kJ mol $^{-1}$  by the  $^{13}\text{C}$  chemical shift anisotropy (CSA) analysis of PC $^{19}$  and 54–56 kJ mol $^{-1}$  by the mechanical relaxation analysis of PC. $^{20,21}$  The same discrepancy was previously reported for the analysis of CSA of PC, $^{19,22}$  and it was already found that the introduction of an inhomogeneous distribution of correlation times was necessary for the analysis. Thus, a distribution of correlation times is introduced to the two-site exchange analysis for the results shown in Figure 4a. For the correlation time distribution, we use Kohlrausch–Williams–Watts (KWW) function $^{23}$

$$\Phi(t) = \exp\left\{-\left(\frac{t}{\tau}\right)^\beta\right\} \quad (2)$$

which is one of the most widely used distribution functions. Here,  $\tau$  is the center of the correlation time, and  $\beta$  controls the breadth of the distribution ( $0 < \beta \leq 1$ ). The simulated line shapes for  $\beta = 0.2$  is shown in Figure 4c. These simulated spectra also reproduce well the experimental spectra in Figure 4a. The temperature dependence of the correlation times of motion thus obtained is shown by half-closed squares in Figure 5. The apparent activation energy, 51 kJ mol $^{-1}$ , agrees with the above-mentioned activation energies for  $\pi$  flip motions for PHR and PC. In contrast, the value of  $\beta = 0.2$  is not consistent with that of  $\beta = 0.6$  for  $^2\text{H}$  NMR line shape analyses of  $\pi$  flip motion in PHR. $^5$  However, the value of  $\beta = 0.2$  seems reasonable because mechanical relaxations and NMR line shape analyses of  $\pi$  flip motion in cured epoxy resins give  $\beta = 0.28^{12}$  and CSA line shape analyses of  $\pi$  flip motion in PC reveal  $\beta = 0.154$ . $^{19}$  Correlation time distributions cannot be deter-



mined uniquely by 1D  $^2\text{H}$  NMR spectra, as is reported previously,<sup>24</sup> and 2D experiments are necessary for the analysis of correlation time distributions.<sup>25,26</sup> Here, 2D CP/MAS exchange experiments are carried out to confirm the value,  $\beta = 0.2$ , as shown later.

The correlation times obtained in this work are reasonably consistent with those by dynamic mechanical analysis<sup>3</sup> (indicated by a closed diamond in Figure 5) and by torsion pendulum<sup>2</sup> (indicated by an open diamond in Figure 5). These correlation times are, however, about 100 times longer than those of Shi's data, which are also included in Figure 5 as open circles. In the above line shape analyses, flip angle distributions are not taken into account. As is indicated by Garroway et al.,<sup>12</sup> analyzed correlation times become shorter by considering flip angle distributions in the analyses of 1D CP/MAS spectra. According to the previous works, flip angle distributions were directly measured by 2D  $^2\text{H}$  NMR experiment in PC<sup>25</sup> and were introduced for the 1D  $^2\text{H}$  NMR line shape analyses in PHR.<sup>5</sup> Thus, the introduction of flip angle distributions seems to be reasonable. In our work, 2D MAS exchange experiments are carried out to confirm the validity of the introduction of flip angle distribution, as shown later.

**Motional Broadening Around  $T_g$  Region.** In Figure 2, the line width of C3–C8 carbons in CP/MAS spectra is found to be almost independent of temperature below 23 °C. Further increase in temperature induces broadening of resonance lines. Such a broadening is known to be caused by enhanced segmental motion. There are two mechanisms for the broadening.<sup>8–11</sup> In one mechanism, the modulation of the  $^{13}\text{C}$ – $^1\text{H}$  dipolar interaction due to molecular motion is interfered with the coherent modulation caused by the applied  $^1\text{H}$  dipolar decoupling when the time scales are similar for the two modulations. In the other mechanism, the modulation of chemical shift anisotropy (CSA) due to molecular motion is interfered with the coherent modulation caused by MAS when the time scales are similar for the two modulations. The temperature region of this motion corresponds to that of the  $\alpha$  relaxation.<sup>3,27</sup> At temperatures higher than 150 °C, the rate of motion exceeds the  $^1\text{H}$  dipolar decoupling field strength and the rotation rate of MAS, and thus, the line width turns out to be narrow again.<sup>17</sup> The line widths of the DD/MAS spectrum at 180 °C are comparable to those in the solution-state spectrum in Figure 1a, where the C7 and C8 resonance lines can be observed separately. It is confirmed that the line broadening at 110–140 °C is caused by main chain motion because such a broadening is observed for main chain C3–C8 carbons. Although no broadening occurs for C1 and C2 carbons, this does not mean that the C1 and C2 carbons do not undergo segmental motion in the temperature range of the  $\alpha$  relaxation. The  $^{13}\text{C}$ – $^1\text{H}$  dipolar widths and the CSA widths of these carbons are expected to be narrow because the C1 carbon undergoes rapid motion around the C1–C2 axis and the C2 carbon is a quaternary carbon. Thus, neither of the above-mentioned two mechanisms works for these carbons.

We can calculate correlation times of the motion associated with the  $\alpha$  relaxation by analyzing the temperature dependence of the line width for each resonance line. When the origin of motional broadening is the modulation of  $^{13}\text{C}$ – $^1\text{H}$  dipolar interaction, the line width of a  $^{13}\text{C}$  resonance line for glassy polymers can be expressed as<sup>8–10</sup>

$$\chi = \chi_0 + \chi_1 \left( 1 + \frac{2}{\pi} \arctan(\alpha(T_0 - T)) \right) + \frac{\lambda M_2}{\pi} \frac{\tau}{1 + \tau^2 \omega_1^2} \quad (3)$$

The first term represents the intrinsic line width due to inhomogeneous static fields, the deviation from the ideal magic angle, etc. The second term empirically expresses the line widths due to a distribution of the isotropic chemical shift arising from inhomogeneous local structures in glassy polymers. The temperature-independent line width below the  $T_g$  region gradually decreases by a parameter  $\alpha$  in the  $T_g$  region due to the averaging of the distribution by molecular motion, and the line width from this contribution becomes  $\chi_1$  at  $T_0$ . The third term expresses the increase in line width due to the motional broadening effect.  $M_2$  is the powder average of the second moment of the  $^{13}\text{C}$ – $^1\text{H}$  dipolar interaction

$$M_2 = \frac{\gamma_{\text{H}}^2 \gamma_{\text{C}}^2 \hbar^2}{5r^6} \quad (4)$$

$r$  is the  $^{13}\text{C}$ – $^1\text{H}$  distance, 0.11 nm, and  $\lambda$  is the reduction factor of the second moment. The decoupling strength,  $\omega_1$ , is  $2\pi \times 50.0$  kHz, as described above.  $\tau$  is the correlation time of molecular motion, and the maximum broadening is observed at  $\omega_1 \tau = 1$ . The Williams–Landel–Ferry (WLF) equation<sup>28</sup> is assumed for the temperature dependence of correlation times

$$\tau = \tau_s \exp \left( \frac{-C_1(T - T_s)}{C_2 + T - T_s} \right) \quad (5)$$

For  $C_1$  and  $C_2$ , we use the typical values at  $T_s = T_g + 50$  °C, 8.86 and 101.6, respectively.<sup>28</sup>  $\tau_s$  is the correlation time at  $T_s$ .

When the origin of motional broadening is the motional modulation of CSA,<sup>11</sup> the third term in eq 3 becomes

$$\frac{2}{15} \omega_0^2 \delta^2 \left( 1 + \frac{\eta^2}{3} \right) \left( \frac{\tau}{1 + 4\tau^2 \omega_r^2} + \frac{2\tau}{1 + \tau^2 \omega_r^2} \right) \quad (6)$$

where  $\delta$  and  $\eta$  are the anisotropy and asymmetry parameters of CSA, respectively. The Larmor frequency,  $\omega_0$ , is  $2\pi \times 100.69$  MHz, and the MAS rotation frequency,  $\omega_r$ , is  $2\pi \times 6000$  Hz.

For the quantitative analysis, the above-mentioned two broadening mechanisms should be considered. The analysis is carried out for C7/8 carbons by using the mechanism of dipolar interaction. Although these two resonance lines cannot be resolved and the line width is estimated as a single line, the  $^{13}\text{C}$ – $^1\text{H}$  dipolar interaction is more than 10 times larger than the CSA width ( $\sim 2$  kHz at 23 °C), and thus, the effect of CSA is reasonably negligible. The analysis is also carried out for the C6 carbon by the mechanism of motional modulation of CSA, since the CSA width ( $\sim 15.6$  kHz at 23 °C) is larger than the  $^{13}\text{C}$ – $^1\text{H}$  dipolar interaction ( $\sim 6$  kHz in the rigid state).

The temperature dependences of the line widths for the C6 and C7/8 carbons are shown in Figure 6. The experimental data for C7/8 carbons are fitted as least-squares fitting by using eqs 3–5. The data for the C6 carbon are subjected to least-squares fitting by using eq 6 instead of the third term of eq 3. The result shown

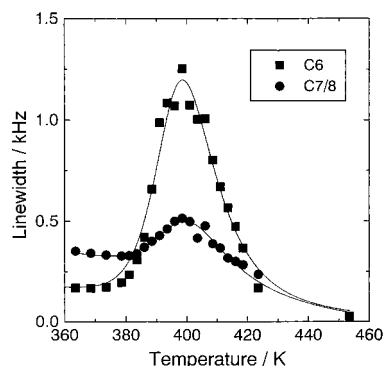


**Figure 6.** Temperature dependence of line widths for the C6 and C7/8 carbons of PHR. The solid curves are the best fit obtained by the least-squares fitting.

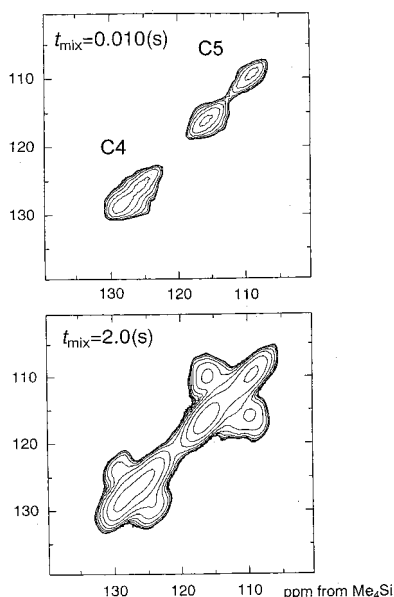


**Figure 7.** 2D CP/MAS  $^{13}\text{C}$  exchange spectra for PHR in the glassy state at  $-120\text{ }^{\circ}\text{C}$ . Only the resonance lines of the phenylene ring C–H carbons are shown. The mixing times are 0.01 and 2.0 s. Contour levels are set to 1,  $1/2$ ,  $(1/2)^2$ , ...,  $(1/2)^n$  from the top level to show smaller intensity signals clearly.

as solid lines in Figure 6 well reproduces the experimental data. The temperature dependences of  $\tau$  thus obtained are also shown in Figure 5 as broken lines (the left and right lines correspond to the results from C6 and C7/8 carbons, respectively). Although there exists a difference between these two lines, which would be originated from the overlap of C7 and C8 resonance lines and the neglect of dipolar interaction effect for the C6 carbon, the result obtained by the following 2D MAS experiment is nearly on the WLF lines obtained here.

**Two-Dimensional CP/MAS  $^{13}\text{C}$  Exchange NMR Spectra.** Figure 7 shows 2D CP/MAS  $^{13}\text{C}$  exchange NMR spectra of PHR at  $-120\text{ }^{\circ}\text{C}$  for mixing times of 10 ms and 2 s. Here, the resonance lines for the C4 and C5 carbons are shown. While the diagonal peaks are observed and the exchange signals are in the noise level for the mixing time of 10 ms, the exchange signals are clearly observed between the two resonance lines for C5 carbons at a mixing time of 2.0 s. The exchange signals are also observed between the two resonance lines for C4 carbons, and no other exchange signals are observed. It can be thus concluded that these exchange signals are not originated from  $^{13}\text{C}$  spin diffusion but the two-site  $\pi$  flip motion; otherwise, exchange signals between

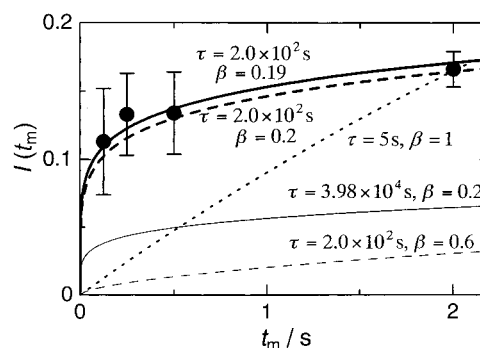


**Figure 8.** Mixing time dependence of exchange intensity for the C5 carbon at  $-120\text{ }^{\circ}\text{C}$ , normalized by the sum intensities of diagonal and exchange signals. Experimental data are shown by solid circles. All the curves follow the eq 7: thick solid line,  $\tau = 2.0 \times 10^2\text{ s}$  and  $\beta = 0.19$ ; thick broken line,  $\tau = 2.0 \times 10^2\text{ s}$  and  $\beta = 0.2$ ; thin solid line,  $\tau = 3.98 \times 10^4\text{ s}$  and  $\beta = 0.2$ ; thin broken line,  $\tau = 2.0 \times 10^2\text{ s}$  and  $\beta = 0.6$ ; dotted line,  $\tau = 5\text{ s}$  and  $\beta = 1$ .

C4 and C5 resonance lines should also appear. The correlation time of this motion at  $-120\text{ }^{\circ}\text{C}$  is analyzed by the mixing time dependence of the exchange signal intensity. Here, it is assumed that the increase of the exchange intensity,  $I(t_m)$ , can be described as KWW type function:

$$I(t_m) = \frac{n-1}{n} \left[ 1 - \exp \left\{ - \left( \frac{t_m}{\tau} \right)^\beta \right\} \right] \quad (7)$$

as was already used for the quantitative analysis of 2D exchange NMR spectra.<sup>26</sup>  $I(t_m)$  is normalized by the total intensity, namely, the sum of diagonal and exchange intensities. The value  $n$  corresponds to the number of the site of motion and the following analyses are carried out with  $n = 2$ .

Figure 8 shows the mixing time dependence of  $I(t_m)$  up to  $t_m = 2.0\text{ s}$ . To determine the parameters,  $\tau$  and  $\beta$ , uniquely, the data at longer  $t_m$  where  $I(t_m)$  reaches an equilibrium value are necessary. At the long  $t_m$  limit, the exchange signal should have the same intensity with the diagonal signal because all the phenylene rings participate in the  $\pi$  flip motion, as is found from 1D CP/MAS spectra. Therefore, it is desirable to carry out the measurements until  $I(t_m)$  becomes 0.5. Experiments for longer  $t_m$  are, however, not performed due to the restrictions of experimental times and spin–lattice relaxation times and to avoid  $^{13}\text{C}$  spin diffusion. The other way is to carry out the measurements at higher temperatures where  $\tau$  becomes shorter. This is true in principle, but the coalescence of resonance lines makes this analysis difficult.

In Figure 8, the calculated  $I(t_m)$  curve with  $\tau = 5\text{ s}$  and  $\beta = 1$  is shown as a dotted line. The experimental data cannot be explained by  $I(t_m)$  curves with any  $\tau$  values when  $\beta = 1$ . The calculated  $I(t_m)$  curve with  $\tau = 2.0 \times 10^2\text{ s}$  and  $\beta = 0.2$  agree well with the experimental data shown by a thick broken line. A thin solid line with  $\tau = 3.98 \times 10^4\text{ s}$  and  $\beta = 0.2$ , which is obtained from the Arrhenius equation for the above-mentioned two-site exchange analyses of 1D CP/MAS spectra (half-closed squares line in Figure 5), is clearly different from the experimental data. The least-squares fitting analysis for the experimental data is carried out, although the result depend on the initial parameter values due to the lack of long  $t_m$  data. The analysis with initial parameters,  $\tau = 2.0 \times 10^2\text{ s}$  and  $\beta = 0.2$ , results in  $\tau =$

$2.0 \times 10^2$  s and  $\beta = 0.19$ , as shown by a thick solid line in Figure 8. The correlation time thus obtained is on the extrapolated line of Shi's data, as shown by a closed triangle in Figure 5. This agreement indicates that the motion analyzed here for the 2D CP/MAS spectra is the  $\pi$  flip motion of the phenylene rings. It also indicates that the argument by Shi et al.<sup>5</sup> for the comparison of  $^2\text{H}$  NMR results and mechanical relaxation data is reasonable.

As shown in Figure 5, the correlation times obtained by  $^2\text{H}$  NMR and 2D CP/MAS results, which are on both the high- and low-temperature sides of 1D CP/MAS data respectively, are shorter than those obtained by the 1D CP/MAS line shape analyses. This indicates that the flip angle of phenylene ring motion is distributed and the elementary step is not an ideal  $\pi$  flip as assumed on the  $^2\text{H}$  NMR analyses.<sup>5</sup> The shifted correlation times, which are obtained by 1D CP/MAS line shape analysis and are shifted according to 2D CP/MAS results, are shown in Figure 5 as closed squares. Now, in turn, the correlation times of the shifted data are deviated from those of mechanical relaxation data.<sup>2,3</sup> The discrepancy is partly solved by the overlap of trans-gauche isomerization of hydroxy ether groups as analyzed by  $^2\text{H}$  NMR experiments.<sup>5</sup>

From Figure 8, it is also found that the calculated  $I(t_m)$  curve with  $\tau = 2.0 \times 10^2$  s and  $\beta = 0.6$ , which is deduced from  $^2\text{H}$  NMR results, is quite different from our experimental 2D data. Therefore, it can be concluded that the value of  $\beta$  is not 0.6 but close to 0.2 at least  $-120$  °C. The temperature-independent KWW exponent,  $\beta$ , is assumed both in the previous  $^2\text{H}$  and our  $^{13}\text{C}$  NMR experiments. However, we cannot deny the possibility that the value of  $\beta$  depends on the temperature, which can reconcile the  $^2\text{H}$  and  $^{13}\text{C}$  NMR results. Actually, our data at 0 and  $-20$  °C are almost insensitive to the value of  $\beta$ , as found from Figure 5 and can be explained by larger  $\beta$  values.

It is also found that all the contour lines of the diagonal peaks in Figure 7 are elliptical. The line width along the diagonal direction, that is, the long axis of the ellipsoid, reflects the distribution of homogeneous lines. This distribution is caused by the disorder in conformation and/or local environments in glassy PHR, which corresponds to the second term of eq 3. The line width perpendicular to the diagonal direction, that is, the short axis of the ellipsoid, corresponds to the homogeneous line width, when there are no exchanges among disordered sites.

When motions are allowed among different conformations or environments in the glassy PHR, exchange signals will appear among the respective homogeneous resonance lines so that the contour line becomes circle. Therefore, the shape of diagonal peaks is found to be indicative of the dynamics in the glassy PHR. The 2D CP/MAS  $^{13}\text{C}$  exchange NMR spectra of PHR between 70 and 90 °C confirms the above discussion. As is found from Figure 9, the diagonal resonance lines of the C3 and C6 carbons are elliptical at 70 °C. With increasing temperature, the line widths perpendicular to the diagonal direction become broader and finally become circular at 90 °C. Here, it should be noted that the inhomogeneous line width is almost independent of temperature below 100 °C (see Figure 6). We can thus conclude that the shape of 2D MAS resonance lines corresponds to the dynamics of the matrix and therefore polymer chains.

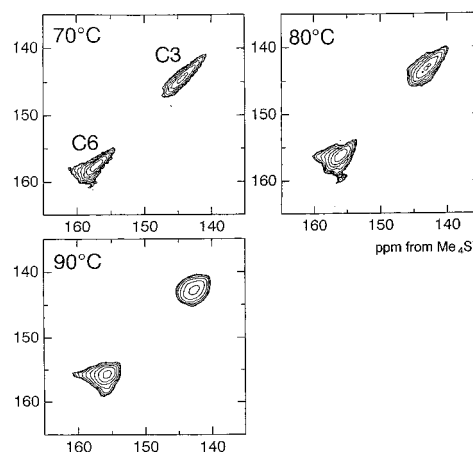


**Figure 9.** 2D CP/MAS  $^{13}\text{C}$  exchange spectra for PHR around the glass transition region (at 70–90 °C). Only the resonance lines of the phenylene ring quaternary carbons are shown. The mixing time is 1.0 s.

The correlation time of main chain motion at 90 °C is phenomenologically analyzed by the mixing time dependence of the line width of 2D CP/MAS  $^{13}\text{C}$  exchange NMR spectra. The correlation time thus obtained, 0.45 s, is plotted in Figure 5 as a closed triangle. This is consistent with the WLF curve obtained by 1D CP/MAS  $^{13}\text{C}$  NMR experiments.

In Figure 7, the cross-peaks are circular, although the diagonal signals are elliptical. This suggests that the local structure is inhomogeneously distributed in space. After one or an odd number of  $\pi$  flip motions, environments of C4 and C5 carbons are different for respective sites; thus, the cross-peaks are not elliptical but circular.

## Conclusion

The dynamics of PHR in the wide temperature range between  $-150$  and  $180$  °C has been analyzed by 1D and 2D MAS  $^{13}\text{C}$  NMR experiments. The resonance lines for C–H carbons of phenylene rings, which split into two lines at  $-150$  °C, coalesce with increasing temperature. The changes of CP/MAS line shapes are originated from phenylene ring  $\pi$  flip motion, and the correlation time of this motion is analyzed on the basis of the two-site exchange model. The temperature dependence of the correlation times is found to follow the Arrhenius equation. The apparent activation energy is  $51 \text{ kJ mol}^{-1}$  by assuming an inhomogeneous correlation time distribution described by a Kohlrausch–Williams–Watts (KWW) function with an exponent of 0.2. The exponent of 0.2 is confirmed by the mixing time dependence of exchange intensities in 2D CP/MAS  $^{13}\text{C}$  exchange NMR experiments at  $-120$  °C. The results of our 1D and 2D CP/MAS experiments are consistent with previous  $^2\text{H}$  NMR results, except for the width of the correlation time distribution.

The  $\alpha$  relaxation for PHR is also analyzed by the motional broadening in MAS  $^{13}\text{C}$  NMR spectra. The temperature dependence of the correlation time can be described by the William–Landel–Ferry (WLF) equation with typical parameters. The shapes of contour lines in 2D CP/MAS experiments also suggest that the local structure of PHR in the glassy state is inhomogeneous.

**Acknowledgment.** The phenoxy resin pellets was kindly supplied by Mr. Ninomiya of UBE Science Co.

Ltd. Computation time was provided by the Super-computer Laboratory, Institute for Chemical Research, Kyoto University. Financial support from a Grant-in-Aid for Encouragement of Young Scientists (11750780), from the Ministry of Education, Science and Culture, Japan, is gratefully acknowledged.

## References and Notes

- (1) del Val, J. J.; Colmenero, J.; Rosi, B.; Mitchell, G. R. *Polymer* **1995**, *36*, 3625.
- (2) Takahama, T.; Geil, P. H. *J. Polym. Sci.: Polym. Phys. Ed.* **1982**, *20*, 1979.
- (3) Erro, R.; Gaztelumendi, M.; Nazabal, J. *J. Polym. Sci. B: Polym. Phys.* **1996**, *34*, 1055.
- (4) Poliks, M. D.; Gullion, T.; Schaefer, J. *Macromolecules* **1990**, *23*, 2678.
- (5) Shi, J.-F.; Inglefield, P. T.; Jones, A. A.; Meadows, M. D. *Macromolecules* **1996**, *29*, 605.
- (6) Kaplan, M. L.; Bovey, F. A.; Chang, H. V. *Anal. Chem.* **1975**, *47*, 1703.
- (7) Tsuji, H.; Horii, F.; Nakagawa, M.; Ikada, Y.; Odani, H.; Kitamaru, R. *Macromolecules* **1992**, *25*, 4114.
- (8) Takegoshi, K.; Hikichi, K. *J. Chem. Phys.* **1991**, *94*, 3200.
- (9) VanderHart, D. L.; Earl, W. L.; Garroway, A. N. *J. Magn. Reson.* **1981**, *44*, 361.
- (10) Rothwell, W. P.; Waugh, J. S. *J. Chem. Phys.* **1981**, *74*, 2721.
- (11) Suwelack, D.; Rothwell, W. P.; Waugh, J. S. *J. Chem. Phys.* **1980**, *73*, 2559.
- (12) Garroway, A. N.; Ritchey, W. N.; Moniz, W. B. *Macromolecules* **1982**, *15*, 1051.
- (13) Nakatsu, K.; Yoshioka, H.; Kunimoto, K.; Kinugasa, T.; Ueji, S. *Acta Crystallogr.* **1978**, *B34*, 2357.
- (14) Steiner, T.; Starikov, E. B.; Tamm, M. *J. Chem. Soc., Perkin Trans.* **1996**, *2*, 67.
- (15) Steiner, T.; Mason, S. A.; Tamm, M. *Acta Crystallogr.* **1997**, *B53*, 843.
- (16) Henrichs, P. M.; Nicely, V. A. *Macromolecules* **1990**, *23*, 3193.
- (17) Abragam, A. *The principles of Nuclear Magnetism*; Clarendon Press: Oxford, 1989.
- (18) Mehring, M. *High-Resolution NMR in Solids*; Springer-Verlag: Berlin, 1983.
- (19) Roy, A. K.; Jones, A. A.; Inglefield, P. T. *Macromolecules* **1986**, *19*, 1356.
- (20) Jho, J. Y.; Yee, A. F. *Macromolecules* **1991**, *24*, 1905.
- (21) Yee, A. F.; Smith, S. A. *Macromolecules* **1981**, *14*, 54.
- (22) O'Gara, J. F.; Jones, A. A.; Hung, C.-C.; Inglefield, P. T. *Macromolecules* **1985**, *18*, 1117.
- (23) Williams, G.; Watts, D. C. *Trans. Faraday Soc.* **1971**, *67*, 1323.
- (24) Horii, F.; Kaji, H.; Ishida, H.; Kuwabara, K.; Masuda, K.; Tai, T. *J. Mol. Struct.* **1998**, *441*, 303.
- (25) Hansen, M. T.; Blumich, B.; Boeffel, C.; Spiess, H. W. *Macromolecules* **1992**, *25*, 5542.
- (26) Wilhelm, M.; Spiess, H. W. *Macromolecules* **1996**, *29*, 1088.
- (27) Alegria, A.; Guerrica-Echevarria, E.; Goitandia, L.; Telleria, I.; Colmenero, J. *Macromolecules* **1995**, *28*, 1516.
- (28) Williams, M. L.; Landel, R. F.; Ferry, J. D. *J. Am. Chem. Soc.* **1955**, *77*, 3701.

MA010444V